

Interaction of selenite with reduced Fe and/or S species: An XRD and XAS study

Nicolas Finck *, Kathy Dardenne

Institute for Nuclear Waste Disposal (INE), Karlsruhe Institute of Technology (KIT), P.O. Box 3640, D-76021 Karlsruhe, Germany

ARTICLE INFO

ABSTRACT

Keywords:
Selenite
Ferrous iron
Sulfide
Mackinawite
XAS

In this study, we investigated the interaction between selenite and either $\text{Fe}^{(\text{II})}_{\text{aq}}$ or $\text{S}^{(-\text{II})}_{\text{aq}}$ in solution, and the results were used to investigate the interaction between $\text{Se}^{(\text{IV})}_{\text{aq}}$ and FeS in suspension. The reaction products were characterized by a combination of methods (SEM, XRD and XAS) and the reaction mechanisms were identified. In a first experiment, $\text{Se}^{(\text{IV})}_{\text{aq}}$ was reduced to $\text{Se}^{(0)}$ by interaction with $\text{Fe}^{(\text{II})}_{\text{aq}}$ which was oxidized to $\text{Fe}^{(\text{III})}$, but the reaction was only partial. Subsequently, some $\text{Fe}^{(\text{III})}$ produced akaganeite (β FeOOH) and the release of proton during that reaction decreased the pH. The pH decrease changed the Se speciation in solution which hindered further $\text{Se}^{(\text{IV})}$ reduction by $\text{Fe}^{(\text{II})}_{\text{aq}}$. In a second experiment, $\text{Se}^{(\text{IV})}_{\text{aq}}$ was quantitatively reduced to $\text{Se}^{(0)}$ by $\text{S}^{(-\text{II})}_{\text{aq}}$ and the reaction was fast. Two sulfide species were needed to reduce one $\text{Se}^{(\text{IV})}$, and the observed pH increase was due to a proton consumption. For both experiments, experimental results are consistent with expectations based on the oxidation reduction potential of the various species. Upon interaction with FeS, $\text{Se}^{(\text{IV})}_{\text{aq}}$ was reduced to $\text{Se}^{(0)}$ and minute amounts of pyrite were detected, a consequence of partial mackinawite oxidation at surface sulfur sites. These results are of prime importance with respect to safe deep disposal of nuclear waste which contains the long lived radionuclide ^{79}Se . This study shows that after release of $^{79}\text{Se}^{(\text{IV})}$ upon nuclear waste matrix corrosion, selenite can be reduced in the near field to low soluble $\text{Se}^{(0)}$ by interaction with $\text{Fe}^{(\text{II})}_{\text{aq}}$ and/or $\text{S}^{(-\text{II})}_{\text{aq}}$ species. Because the solubility of $\text{Se}^{(0)}$ species is significantly lower than that of $\text{Se}^{(\text{IV})}$, selenium will become much less (bio)available and its migration out of deep HLW repositories may be drastically hindered.

1. Introduction

Selenium occurs in nature as trace element and as for many elements, it is an essential nutrient for animals and humans, but is toxic at elevated concentrations (Fernández Martínez and Charlet, 2009). The chemical speciation and thus the solubility of Se in natural systems depend to a large extent on pH and E_h conditions. Under oxidizing conditions, Se occurs as mobile hexavalent (SeO_4^{2-}) and tetravalent (SeO_3^{2-}) oxyanions, whereas it forms low soluble $\text{Se}^{(0)}$ and $\text{Se}^{(-\text{II})}$ solids under reducing conditions. The oxidized species also show a higher chemical

toxicity (Fernández Martínez and Charlet, 2009) and are considered more mobile in subsurface environments than the reduced species (Masscheleyn et al., 1990). Additionally, the geochemistry of Se is also largely controlled by that of iron, with which Se is closely affiliated in both oxidizing and reducing environments (Hatten, 1977).

Selenium is also produced in nuclear power plants by fission of ^{235}U . The long lived and radioactive isotope ^{79}Se (half life of 3.27×10^5 years (Jörg et al., 2010)) present in the high level nuclear waste (HLW) is considered one of the dose dominant nuclides in safety assessment calculations. Recent studies showed that selenium is present in tetravalent oxidation state in HLW glass (Dardenne et al., 2015). Upon HLW glass corrosion by groundwater in deep repositories, mobile selenite species may thus be released and possibly

* Corresponding author.
E-mail address: nicolas.finck@kit.edu (N. Finck).

migrate to the far field. However, reducing conditions are expected to develop in e.g. clay based repository systems (Gaucher et al., 2006) that may reduce Se^(IV) to lower oxidation state(s). The presence of reduced Fe^(II) and/or S^(-II) species as accessory minerals (e.g., pyrite) also buffers the redox milieu.

Dissolved Fe^(II)_{aq} and S^(-II)_{aq} are expected to be present in deep disposal sites and may have a capacity to reduce Se^(IV) similar to that of S^(-II) or Fe^(II) containing solids. The contact of groundwater with canisters containing HLW will result in steel corrosion, thereby releasing Fe^(II)_{aq} species and producing H₂. Studies showed that Fe^(II) bearing solids form as secondary phases upon steel corrosion in the presence of clay or clay pore water and that a significant fraction of Fe^(II)_{aq} migrates away from the corroding surface (e.g., (Schlegel et al., 2014)). It was also suggested that this Fe^(II)_{aq} fraction could favor reduction and immobilization of redox sensitive radionuclides. Furthermore, the production of H₂ will also very likely improve the conditions for microbial activity (Libert et al., 2011). Specifically, H₂ will constitute an energetic substrate for anaerobic bacterial communities and strongly stimulate reducing reactions involving e.g., sulfates (Libert et al., 2014). The presence of reduced sulfur species (e.g., S^(-II)) in repository surroundings is thus very likely. Both ferrous iron and sulfide species may be present in a HLW repository surrounding, and each species can provide electrons to reduce Se^(IV), thereby significantly lowering the selenium solubility and thus its migration. Reactions involving only two reacting species, where only one can be oxidized and only one can be reduced, can be investigated in great detail more easily than reactions involving various reduced species. Information obtained by investigating simple systems can subsequently be used to study more complex systems where more than one species (e.g., Fe^(II) and S^(-II) in FeS) can reduce redox sensitive elements. Unfortunately, only very few investigations have reported on the interaction of Se^(IV) with either Fe^(II)_{aq} or S^(-II)_{aq}.

From a thermodynamic viewpoint, the standard reduction potential of sulfides species are lower than that of selenite species (Table 1), meaning that S^(-II)_{aq} can reduce Se^(IV)_{aq} in an aqueous phase. For example, two sulfide species, each providing two electrons, are needed to reduce one selenite species to its elemental state. Pettine et al. (2012)) reported

Table 1

Table of selected aqueous species formal potentials (Cornell and Schwertmann, 1996; Bouroushian, 2010) and protonation constants (Olin et al., 2005).

Half-reaction	Formal potential (V vs S.H.E. at 25 °C)
SeO ₃ ²⁻ + 6H ⁺ + 4e ⇌ Se(s) + 3H ₂ O	+0.875
HSeO ₃ + 5H ⁺ + 4e ⇌ Se(s) + 3H ₂ O	+0.778
Fe ³⁺ + e ⇌ Fe ²⁺	+0.770
H ₂ SeO ₃ + 4H ⁺ + 4e ⇌ Se(s) + 3H ₂ O	+0.740
S(s) + 2H ⁺ + 2e ⇌ H ₂ S(aq)	+0.141
S(s) + H ⁺ + 2e ⇌ HS ⁻	0.065
S(s) + H ₂ O + 2e ⇌ HS ⁻ + OH ⁻	0.52
S(s) + 2e ⇌ S ²⁻	Available values range from 0.45 to 0.58 V, most probable close to 0.48 V.
Protonation reaction	
SeO ₃ ²⁻ + H ⁺ ⇌ HSeO ₃	Protonation constant log ₁₀ K ⁰ = 8.36 ± 0.23
HSeO ₃ + H ⁺ ⇌ H ₂ SeO ₃	log ₁₀ K ⁰ = 2.64 ± 0.14

rates for the reduction of Se^(IV) by sulfide, however without structural characterization (i.e., XRD) of formed solid phases. Depending on the chemical conditions, the formation of selenium sulfide or a mixture of elemental selenium and colloidal sulfur particles has also been reported (Geoffroy and Demopoulos, 2011). Unfortunately, these reported studies have been performed under aerobic conditions, and reduced sulfur species can be readily oxidized by oxygen present in the air. Because anoxic conditions will develop during the evolution of a HLW disposal site, additional studies performed in the absence of oxygen are needed in order to be useful for safety performance calculations.

The reduction of Se^(IV)_{aq} by Fe^(II)_{aq} species is more complex. The standard reduction potential of the Fe^(III)/Fe^(II) couple is higher than that of sulfide (Table 1) and of comparable value than that of the Se^(IV) species. The ability of Fe^(II) to reduce Se^(IV) is governed by the speciation in solution. For example, HSeO₃⁻ can be reduced by Fe^(II) but H₂SeO₃ cannot because of its lower reduction potential. Also, four electrons are needed to reduce one selenite species, i.e., four Fe^(II) species must each provide one electron for the reduction of one Se^(IV) species. The likelihood of such five species in close proximity in solution in the absence of any mineral surface may be low and if the reaction occurs, it may rapidly slow down because the Fe^(II)_{aq} concentration decreases four times faster than that of Se^(IV)_{aq}. In fact, the ability of Fe^(II)_{aq} to reduce Se^(IV)_{aq} was questioned by several authors. For example, Chen et al. (2009)) failed to reduce Se^(IV)_{aq} by ferrous iron in the absence of reactive surface even though Fe^(II)_{aq} was in large excess at pH < 5.6. Similarly, Charlet et al. (2007)) failed to reduce Se^(IV) but observed the formation of FeSeO₃ by mixing Se^(IV)_{aq} and Fe^(II)_{aq} with a molar ratio of 1:1 at pH 5. The formed solid phase was poorly crystalline (no diffraction data shown); Mossbauer data indicated that half of Fe^(II) was oxidized and based on XAS data ~25% Se was reduced after 4 h. Spectroscopic data were consistent with the formation of a nanoparticulate precipitate where surface Fe atoms are oxidized while Se atoms remain 4 fold coordinated by oxygen atoms as is typical for selenite. In these studies, the presence of a mineral surface acted like a catalyzer, meaning that Se^(IV) was reduced to Se⁽⁰⁾ in the presence of either iron oxides (Chen et al., 2009) or the clay mineral montmorillonite (Charlet et al., 2007). In the present study, the reactivity of Se^(IV) in the presence of a large excess of Fe^(II) (Fe:Se molar ratio of 4:1) was investigated under anoxic conditions and in the absence of mineral phases.

At ambient temperature and pressure, mackinawite (FeS) is the primary precipitate formed by reaction between Fe^(II)_{aq} and S^(-II)_{aq} (Rickard et al., 2006). Mackinawite is a highly reactive phase and was used as a substrate in adsorption studies of various actinides such as Np^(V) (Moyes et al., 2002) or Pu^(V) (Kirsch et al., 2011). Studies on the interaction of Se^(IV) with mackinawite have also been reported (Scheinost and Charlet, 2008; Scheinost et al., 2008) and indicated an influence of the chemical conditions on the nature of the formed Se species. However, in these experiments, the contact time was at maximum 1 day and for such rather short contact times kinetically slow reactions can be easily overlooked. In the present study, Se^(IV) was contacted with pre formed mackinawite in suspension for several days before spectroscopic analysis of the sample.

The goal of this study was to investigate the interaction between $\text{Se}^{(\text{IV})}_{\text{aq}}$ and either $\text{Fe}^{(\text{II})}_{\text{aq}}$ or $\text{S}^{(-\text{II})}_{\text{aq}}$, and to use these results to identify the possible mechanism of interaction between $\text{Se}^{(\text{IV})}_{\text{aq}}$ and FeS. The nature of the reaction products was characterized by scanning electron microscopy (SEM) and X ray diffraction (XRD), and information on the Se speciation was provided by X ray absorption spectroscopy (XAS). We performed investigations under defined conditions in the laboratory to demonstrate that the reduction of $\text{Se}^{(\text{IV})}_{\text{aq}}$ by either $\text{Fe}^{(\text{II})}_{\text{aq}}$ or $\text{S}^{(-\text{II})}_{\text{aq}}$ in solution can operate. Because the presence of mineral surfaces is not expected to hinder the reaction mechanism(s), it can be anticipated that similar mechanism may operate in a HLW surrounding when the same species are present.

2. Materials and methods

2.1. Sample preparation

All samples were prepared with ultra pure water (18.2 M $\Omega \cdot \text{cm}$, Milli Q system (Millipore)) and reagents of ACS grade or higher. All experiments were performed under anoxic conditions, from sample preparation (in an Ar filled glove box) to sample analysis. All solutions and suspensions were purged with Ar for several hours before bringing them into the Ar filled glove box where they were allowed to outgas for at least overnight prior to use. Solutions of $\text{Fe}^{(\text{II})}$ and $\text{S}^{(-\text{II})}$ were freshly prepared before every experiment by dissolving $\text{Fe}(\text{NH}_4)_2(\text{SO}_4)_2 \cdot 6\text{H}_2\text{O}$ or $\text{Na}_2\text{S} \cdot 9\text{H}_2\text{O}$, and the source of $\text{Se}^{(\text{IV})}$ was Na_2SeO_3 . pH and E_h were allowed to drift freely, and values were recorded in suspension before samples were filtered (0.45 μm pore size diameter) for analysis of the solid phases.

The sample SeFerrous was prepared by the addition of a $\text{Se}^{(\text{IV})}$ solution (adjusted to pH 5 by the addition of HCl) into a $\text{Fe}^{(\text{II})}$ solution under stirring (molar ratio Se:Fe = 1:4). A solid phase formed rapidly and red particles were present in suspension after 4 days of reaction. Final pH and E_h were 2.84(5) and +165(30) mV vs Ag/AgCl, respectively. Sample SeSulfide was prepared by drop by drop addition of a $\text{Se}^{(\text{IV})}$ solution into a $\text{S}^{(-\text{II})}$ solution under stirring (molar ratio Se:S = 1:2). Red particles formed very rapidly. After 3 h of reaction, the suspension was filtered and the supernatant was pale yellow. Final pH and E_h were 13.29(5) and -500(30) mV vs Ag/AgCl, respectively. For the last sample (SeMack), mackinawite was first precipitated by mixing $\text{Fe}^{(\text{II})}$ and $\text{S}^{(-\text{II})}$ solutions under stirring, filtered (0.45 μm pore size) after few minutes and washed with water to remove excess ions, and re-suspended in water (at this stage, pH and E_h were 7.25(5) and -600(30) mV vs Ag/AgCl, respectively). A selenite solution was added to the FeS suspension under stirring ($\text{m/V} = 10 \text{ g/L}$ FeS, $[\text{Se}^{(\text{IV})}] = 13 \text{ mmol/L}$). After 7 days of reaction, the measured pH and E_h were 11.50(5) and -570(30) mV vs Ag/AgCl, respectively.

2.2. Structural and spectroscopic characterizations

Solid phases were characterized by SEM and XRD. Information on the size and morphology was obtained by SEM (CamScan CS44FE). Samples were prepared in the Ar filled glove box, transported under anoxic conditions (closed vessel) and quickly positioned in the microscope

to minimize the exposure time to air. Solid phases were identified by recording X ray diffractograms. A small amount of sample slurry was allowed to dry on an air tight sample holder in the Ar filled glove box and used to record XRD data on a D8 Advance (Bruker) diffractometer (Cu K_α radiation) equipped with an energy dispersive detector (Sol X). Phases were identified by comparison with the PDF 2 database.

Information on the Se speciation was obtained by X ray absorption spectroscopy (XAS). In the XANES region, the edge energy increases with the formal oxidation state due to increased effective nuclear charge as valence electrons are removed. Additionally, the edge, formally assigned to a $1s \rightarrow 4p$ transition, gains intensity as valence increases, which is attributable to a decrease in population of the valence $4p$ levels (Pickering et al., 1995). Information on the local chemical environment was obtained by fits to the EXAFS data. Selenium K edge XAS spectra were collected at the INE Beamline (Rothe et al., 2012) for actinide science at the synchrotron light source ANKA (Karlsruhe, Germany). The storage ring energy was 2.5 GeV and the ring current was 180 90 mA. Energy calibration was done by assigning the first inflection point of the Se K edge of a Se foil at 12,658.0 eV and this reference was measured in parallel with all samples. Samples were mounted in the Ar filled glove box into an air tight cell allowing measurements under anoxic conditions. Data were collected in transmission mode or in fluorescence mode using a 5 element LEGe solid state detector (Canberra Eurisys). Data were analyzed following standard procedures by using Athena and Artemis interfaces to the Ifeffit software (Ravel and Newville, 2005). EXAFS spectra were extracted from the raw data and Fourier transforms (FTs) were obtained from the $k^2 \cdot \chi(k)$ functions. Data were fit in R space by using a combination of single scattering paths where phase and amplitude functions for each path were calculated separately with feff8.4 (Ankudinov et al., 1998). Uncertainties on coordination numbers and bond distances are indicated in brackets in Table 2. The fit quality was quantified by the R_f factor, as reported in Finck et al. (2015), representing the absolute misfit between theory and experimental data. Reference XAS data were collected in transmission mode for FeSe, $\text{Se}^{(0)}$ and Na_2SeO_3 .

3. Results and discussion

3.1. Sample SeFerrous

The $\text{Se}^{(\text{IV})}$ solution was adjusted to pH 5 before the addition of $\text{Fe}^{(\text{II})}$ in order to avoid $\text{Fe}(\text{OH})_2(\text{s})$ precipitation and thus the interaction of selenite with this phase. This reaction was investigated by Zingaro et al. (1997) who showed a reduction of selenite and selenate to elemental Se. In the present study, mixing $\text{Se}^{(\text{IV})}$ and $\text{Fe}^{(\text{II})}$ solutions formed red particles shortly after mixing, which hints at the rapid formation of $\text{Se}^{(0)}$. The presence of $\text{Se}^{(0)}$ was corroborated by XRD analysis (Fig. 1), and the presence of additional $\text{Se}^{(\text{IV})}$ compounds ($\text{Fe}_2(\text{SeO}_3)_3 \cdot \text{H}_2\text{O}$ and Na_2SeO_3) indicates that the reduction was only partial, despite the molar ratio of Se:Fe = 1:4. In this system, $\text{Se}^{(\text{IV})}$ can only be reduced by oxidation of $\text{Fe}^{(\text{II})}$. The oxidation of $\text{Fe}^{(\text{II})}$ to $\text{Fe}^{(\text{III})}$ is indicated by the presence of

Table 2

Se K-edge energy position of the XANES and results from EXAFS data fitting.

Sample	E^0 [eV]	Coordination shells			ΔE^0 [eV]	R_f
		N	R [Å]	σ^2 [Å ²]		
Na ₂ Se ^(IV) O ₃ Se ⁽⁰⁾ trigonal	12,662.4	3.0(3) O	1.71(2)	0.002	19.8	0.020
	12,658.0	2.0(2) Se	2.37(2)	0.004		
		4.0(4) Se	3.40(3)	0.020	10.8	0.004
		2.0(4) Se	3.71(3)	0.013		
FeSe ^(II)	12,657.2	1.9(2) Fe	2.39(2)	0.004	7.7	0.002
		0.2(1) Se	2.78(2)	0.003		
		1.6(3) Se	3.71(2)	0.009		
		1.9(4) Se	3.97(3)	0.009		
		1.3(4) Fe	4.51(4)	0.009		
		3.0(2) O	1.69(2)	0.001		
SeFerrous	12,662.6	5.0(5) O	3.30(2)	0.002	12.4	0.018
		2.2(4) Fe	3.50(3)	0.002		
		5.2 (1.9) O	3.69(4)	0.002		
		2.4(2) Se	2.38(2)	0.005		
		0.7(2) Se	3.36(2)	0.005		
SeSulfide	12,657.9	2.8(3) Se	2.36(2)	0.007	8.1	0.010
		1.1(3) Se	3.30(2)	0.007		
SeMack	12,658.0	0.6(2) S	3.87(4)	0.002		

E^0 : energy position of the XANES, N : coordination number, R : interatomic distance, σ^2 : mean square displacement ("Debye-Waller" term), ΔE^0 : shift in ionization energy, R_f : figure of merit of the fit.

akaganeite (β FeOOH) and $(\text{NH}_4)_3\text{Fe}(\text{SO}_4)_3$. The presence of Fe^(II) compound ($\text{Na}_2\text{Fe}(\text{SO}_4)_2 \cdot 4\text{H}_2\text{O}$) corroborates that the reaction was not quantitative. Except Se⁽⁰⁾ and akaganeite, the compounds identified in the diffractogram certainly

formed during sample drying. SEM analysis indicates the presence of particles of various not well resolved shapes having sizes ranging from several hundreds of nanometers up to one micrometer (Fig. 2).

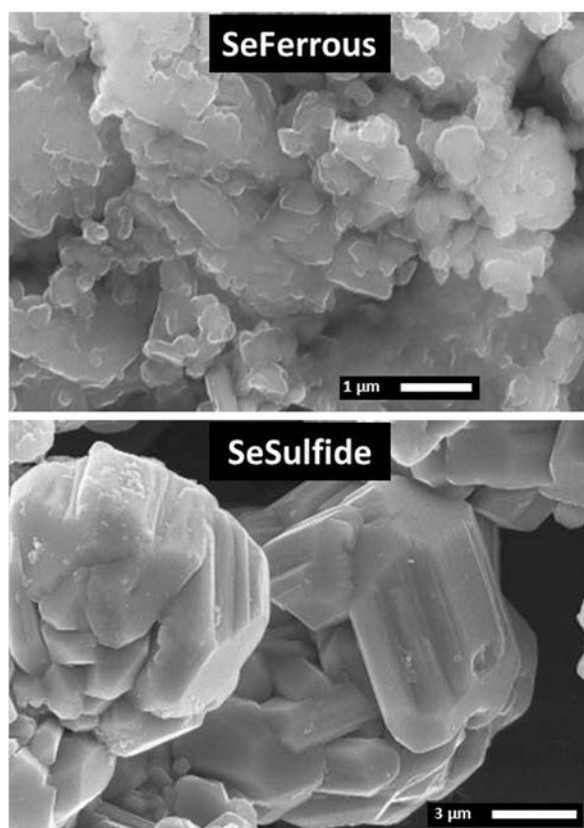


Fig. 1. SEM picture of the samples SeFerrous (top) and SeSulfide (bottom).

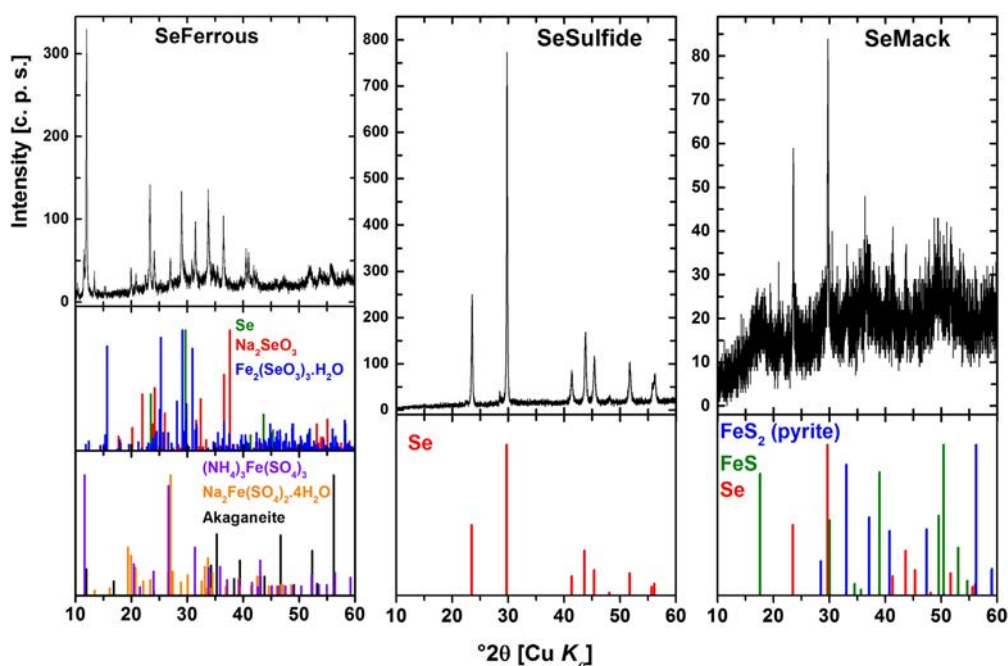


Fig. 2. X-ray diffractogram with peak identification for SeFerrous (left panel), SeSulfide (middle panel) and SeMack (right panel).

Information on the Se speciation was provided by probing the *K* edge by XAS. Compared to the reference compounds, the position and the height of the edge indicate the presence of $\text{Se}^{(\text{IV})}$ in SeFerrous (Fig. 3). This is also clearly seen from the position of the first derivative (inset in Fig. 3). Additionally, the presence of small amounts of $\text{Se}^{(0)}$ is evidenced from a maximum on the lower energy side of the first derivative. The simultaneous presence of $\text{Se}^{(0)}$ and $\text{Se}^{(\text{IV})}$ species is consistent

with XRD data. According to the intensities of the maxima of the first derivative, $\text{Se}^{(0)}$ represents only a minor amount of total Se. In the EXAFS regime, the spectrum of SeFerrous looks very similar to that of the $\text{Se}^{(\text{IV})}$ reference, in agreement with XANES data. The FT contains a first peak at $R + \Delta R \sim 1.3 \text{ \AA}$ and two additional peaks centered around $R + \Delta R \sim 3 \text{ \AA}$ (Fig. 3). A good fit to the data was provided considering a first O shell at $R_{\text{Se-O1}} = 1.69(2) \text{ \AA}$ containing $N_{\text{O1}} = 3.0(2)$ atoms (Table 2).

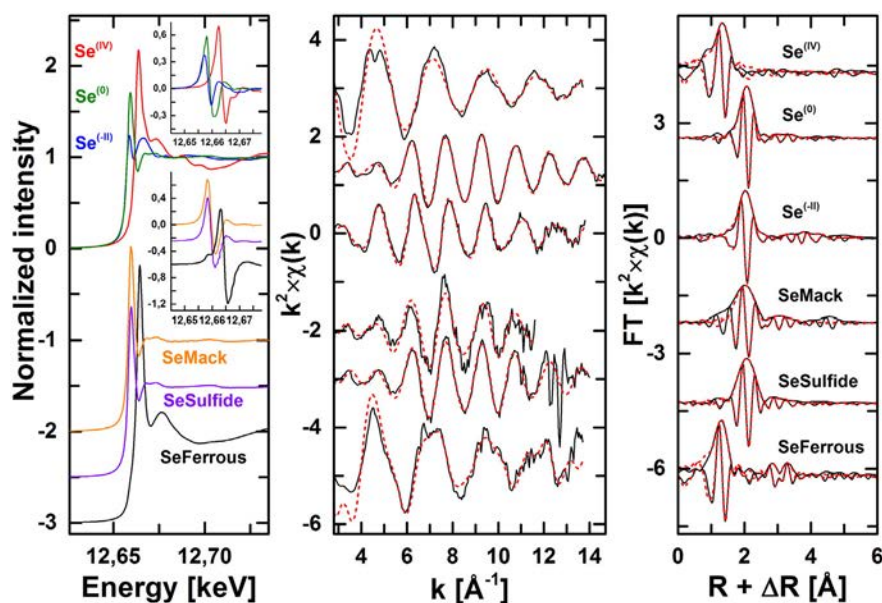


Fig. 3. Se *K*-edge XAS of the samples and of the reference compounds: XANES data in the left panel (insets show the first derivatives), experimental (solid black lines) and modeled (dashed red lines) spectra in the middle panel and the corresponding Fourier transforms in the right panel. The metrical fit results are presented in Table 2.

These distance and coordination number are characteristics of a selenite unit, which are consistent with the phases detected by XRD (sodium and iron selenite). Additional O ($R_{\text{Se-O}2} = 3.30(2) \text{ \AA}$ and $R_{\text{Se-O}3} = 3.69(4) \text{ \AA}$) and Fe ($R_{\text{Se-Fe}1} = 3.50(3) \text{ \AA}$) shells were used to fit higher distance peaks (Table 2). The detected Fe and O shells are consistent with reported crystallographic data of $\text{Fe}_2(\text{SeO}_3)_3 \cdot \text{H}_2\text{O}$ (Giester, 1993), which was detected by XRD. XRD indicated the presence of $\text{Se}^{(0)}$ but no neighboring Se could be detected by XAS. This result is consistent with XANES data indicating that only a small fraction of Se is present as $\text{Se}^{(0)}$. Bond distances of $R_{\text{Se-O}} = 1.69 \text{ \AA}$ and $R_{\text{Se-Fe}} = 3.35 \text{ \AA}$ have been reported for FeSeO_3 (Charlet et al., 2007). Compared to these reported values, the oxygen shell is detected at similar distance, but the Fe shell is located at larger distance in this study, ruling out the presence of FeSeO_3 in SeFerrous. The absence of this phase is also consistent with XRD data and can be explained by the initial chemical conditions in this study differing from that in (Charlet et al., 2007).

At the end of experiment, slightly oxidizing and acidic conditions prevailed in suspension. XAS data indicate that some selenite was reduced to $\text{Se}^{(0)}$, implying the oxidation of four $\text{Fe}^{(II)}$ to $\text{Fe}^{(III)}$. The following equation may explain the mechanism: $4\text{Fe}^{2+} + \text{HSeO}_3^- + 5\text{H}^+ \rightarrow 4\text{Fe}^{3+} + \text{Se}^{(0)} + 3\text{OH}^-$. However, this reaction implies a consumption of protons and a production of OH^- that would increase the pH, in contrast to observations. Yet, the presence of akaganeite was indicated by XRD. The presence of Cl^- , from HCl used to adjust the pH, certainly initiated the formation of akaganeite following: $\text{Fe}^{3+} + 2\text{H}_2\text{O} \rightarrow \text{FeOOH} + 3\text{H}^+$ (Schwertmann and Cornell, 1991). In that reaction 3 protons are formed for one reacting ferric iron and, consequently, the reduction of $\text{Se}^{(IV)}$ by $\text{Fe}^{(II)}$ results in an overall pH decrease, which is consistent with the experimental results. Additionally, some $\text{Fe}^{(III)}$ also formed $\text{Fe}_2(\text{SeO}_3)_3 \cdot \text{H}_2\text{O}$, as indicated by XRD and XAS data.

In acidic medium, selenite is protonated and present as H_2SeO_3 or HSeO_3^- . In SeFerrous, pH (2.84(5)) is close to pK_{a1} ($\text{pK}_{a1} = 2.64 \pm 0.16$, Table 1) meaning that a large fraction of Se is present as doubly protonated species and the remaining as a singly protonated species. Furthermore, the reduction potential of $\text{H}_2\text{SeO}_3/\text{Se}$ ($E^0 = +0.740 \text{ V}$) is lower than that of $\text{Fe}^{(III)}/\text{Fe}^{(II)}$ ($E^0 = +0.770 \text{ V}$) indicating that the reduction is thermodynamically not possible. In contrast, the reduction of HSeO_3^- ($E^0 = +0.778 \text{ V}$) is possible. Consequently, it is very likely that the addition of $\text{Se}^{(IV)}$ into $\text{Fe}^{(II)}$ initially reduced selenite to $\text{Se}^{(0)}$ with a concomitant oxidation of $\text{Fe}^{(II)}$ to $\text{Fe}^{(III)}$. Akaganeite formed rapidly and induced a decrease in pH which in turn changed the Se speciation, inhibiting further $\text{Se}^{(IV)}$ reduction. This explanation is consistent with the presence of both $\text{Se}^{(IV)}$ and $\text{Se}^{(0)}$ compounds, as well as $\text{Fe}^{(II)}$ and $\text{Fe}^{(III)}$ compounds. Additionally, the $\text{Fe}^{(II)}$ content decreased four times faster than $\text{Se}^{(IV)}$, making the reaction less likely because in dilute systems the probability of four $\text{Fe}^{(II)}$ to come close enough to enable $\text{Se}^{(IV)}$ reduction to take place is lower than in systems with higher concentrations.

The prevalence of slightly oxidizing conditions ($E_h = +165(30) \text{ mV}$ vs Ag/AgCl) may be less easy to explain. The reduction potential is determined by the transfer of electrons between chemical species, that is, it represents how strong electrons are transferred to or from species in solution. In SeFerrous, no attempt was made to impose pH or E_h , and thus

the E_h value adjusted itself. It indicates only a weak tendency to exchange electrons between chemical species.

The data show that $\text{Se}^{(IV)}$ can be reduced by $\text{Fe}^{(II)}$, as long as the Se speciation does not render the reaction thermodynamically impossible. In deep disposal sites, prevailing pH should be around neutral, and thus the Se speciation is expected to be dominated by HSeO_3^- , at least before becoming reducing due to radioactive decay. The presence of mineral phases (e.g., clay minerals, quartz, iron oxides) will also possibly mediate the reduction (Charlet et al., 2007; Chen et al., 2009) of selenite to $\text{Se}^{(0)}$ by $\text{Fe}^{(II)}$. Because $\text{Se}^{(0)}$ is less soluble, i.e., less mobile than selenite, it is very likely that selenium will be immobilized in the near field and not migrate out of the repository site.

3.2. Sample SeSulfide

Mixing selenite and sulfide solutions leads to a rapid $\text{Se}^{(IV)}$ reduction to $\text{Se}^{(0)}$. The reaction is thermodynamically possible (Table 1) and the oxidation of sulfide provided the electrons needed to reduce selenite. Trigonal selenium was detected as main crystalline phase by XRD, and the small peak at $\sim 28.5^\circ 2\theta$ may possibly correspond to a minor mixed chalcogenide phase of composition $\text{Se}_{3.3}\text{S}_{4.7}$ (Weiss, 1977). The electron micrograph of SeSulfide (Fig. 2) indicates the presence of aggregates consisting of crystals of several micrometers in size.

The intensity and the position of the XANES both indicate the presence of $\text{Se}^{(0)}$ (Fig. 3). No $\text{Se}^{(IV)}$ could be detected indicating that the reaction was quantitative. The EXAFS spectrum looks similar to that of the $\text{Se}^{(0)}$ reference, consistent with the XANES result. A good fit to the EXAFS data was provided considering two neighboring Se shells at $R_{\text{Se-Se}2} = 2.38(1) \text{ \AA}$ and $R_{\text{Se-Se}2} = 3.36(2) \text{ \AA}$, and containing ~ 2 atoms and ~ 1 atom, respectively (Table 2). The Se1 shell is within uncertainty identical to the $\text{Se}^{(0)}$ reference and to reported crystallographic data (2 atoms located at $R_{\text{Se-Se}1} = 2.38 \text{ \AA}$ (Cherin and Unger, 1967)), and the Se2 shell is reasonably close to reported data for trigonal Se (4 Se at $R_{\text{Se-Se}2} = 3.44 \text{ \AA}$). No other backscatterer could be detected, meaning that if another phase (crystalline or amorphous) is present, it only represents a marginal amount.

Sulfide was oxidized and selenite was reduced, consistent with thermodynamic (Table 1) and XRD data. The most plausible mechanism is the oxidation of $\text{S}^{(-II)}$ to $\text{S}^{(0)}$ whereby two sulfide ions were used to reduce one $\text{Se}^{(IV)}$ species. The reaction was also accompanied by a clear increase in pH that may originate from a consumption of proton and/or a formation of OH^- . The following reaction would be consistent with the experimental chemical conditions: $\text{HSeO}_3^- + 2\text{S}^{2-} + 5\text{H}^+ \rightarrow \text{Se}^{(0)} + 2\text{S}^{(0)} + 3\text{H}_2\text{O}$. The presence of elemental selenium is corroborated by XRD and XAS data. Unfortunately $\text{S}^{(0)}$ could not be detected by XRD, however it may prevail as a separate X ray amorphous phase or it may be present as dissolved species in the filtrate. The filtrate was not analyzed and thus the hypothesis of the presence of dissolved or nanoparticulate $\text{S}^{(0)}$ species cannot be corroborated, but the yellow color is diagnostic of elemental sulfur. Consequently, the equation accounts best for the experimental results and thus the pH increase is due to a consumption of protons. Additionally, the large difference in reduction potential (Table 1) between selenite and sulfide species may explain that

the reaction was fast. Electrons were exchanged readily in that sample, thus explaining that reducing conditions developed.

The data indicate a fast reaction between dissolved selenite and sulfide, even in the absence of mineral surface. Only two $S^{(-II)}$ species are needed to reduce one $Se^{(IV)}$ species and the likelihood of having these three species close enough to react is larger than the five species needed in SeFerrous. The outcomes indicate that selenite can be reduced upon interaction with sulfide in a disposal site, thus warranting Se immobilization.

3.3. Sample SeMack

Studies on the interaction between selenite and mackinawite in suspension can be found in the literature (Scheinost and Charlet, 2008; Scheinost et al., 2008). The main difference between both studies was the sample preparation: in one study the substrate was washed to establish a defined ionic strength (Scheinost et al., 2008) whereas the substrate was not conditioned in the second (Scheinost and Charlet, 2008). Based on the sample preparation, the present study compares well with the latter (Scheinost and Charlet, 2008). In this reported study, the pH increased from 6.3 to 9.7 after one day of reaction and only $Se^{(0)}$ was detected. However, a much longer contact time was considered in the present study (7 days).

The X ray diffractogram of the solid phase in SeMack is noisy, but several phases can be identified. The substrate (FeS) was identified as mackinawite mainly from the broad peaks at ~ 17.6 and $50.5^\circ 2\theta$ (Lennie et al., 1995), and the diffractogram also compares well with published data (Finck et al., 2012). The width of the peaks indicates that FeS is of nanoparticulate size and thus exhibits a large specific surface area. For similar synthesis procedure, particle sizes of < 10 nm have been reported with a surface area of up to several hundreds m^2/g (Wolthers et al., 2003; Scheinost et al., 2008). Considering an average of 4 sites/ nm^2 (Wolthers et al., 2005), the monolayer surface coverage was not reached in SeMack: 10 g/L FeS considering 100 m^2/g yield 0.4 mol/L surface sites, which is much larger than the Se concentration of 13 mmol/L. Elemental selenium (trigonal phase) was also identified on the X ray diffractogram, and small amounts of pyrite (FeS_2) (Brostigen and Kjekshus, 1969) could be detected, mainly from the small peaks at ~ 33.1 and $37.1^\circ 2\theta$.

The XANES indicates that Se is present as $Se^{(0)}$ and thus $Se^{(IV)}$ was reduced. Though noisy, the EXAFS data look similar to that of the $Se^{(0)}$ reference compound. A good fit to the data was provided considering Se backscatterers at 2.36(1) Å and 3.30(2) Å, and an additional possible S shell at $R_{Se-S1} = 3.87(4)$ Å containing < 1 atom (Table 2). The detected Se backscatterers are consistent with the presence of $Se^{(0)}$ and the S shell can be interpreted as originating from the substrate surface (FeS and/or FeS_2). The formation of $Se^{(0)}$ is consistent with previous finding (Scheinost and Charlet, 2008), but no S shell was detected in that study.

XAS data indicate that $Se^{(IV)}$ was reduced, meaning that $Fe^{(II)}$ and/or $S^{(-II)}$ from the substrate was oxidized. XRD data indicate that FeS and FeS_2 are present in the sample, pyrite representing only a minor constituent. The presence of this compound can be explained by a partial FeS oxidation at the surface during the reductive immobilization of selenite. Specifically, the oxidation state of sulfur likely increased from $-II$ to $-I$. At the beginning of the experiment, pH = 7.25 was

close to the reported point of zero charge (PZC) of ~ 7.5 (Wolthers et al., 2005). It was also proposed that the surface of hydrated mackinawite can best be described at pH $< \sim 10$ by mono coordinated ($\equiv FeS$) and tri coordinated ($\equiv Fe_3S$) sulfide functional groups, the former determining the acid base properties at pH $< PZC$ and the latter at higher pH. Consequently, $Se^{(IV)}$ interacted with the substrate at sulfide sites, rather than at iron hydroxyl groups, and thus these groups underwent oxidation to form FeS_2 , consistent with XRD data. Additional evidence of the reduction at the sulfur sites comes from the increase in pH, a variation similar to that observed in SeSulfide, but not in SeFerrous. The oxidation of surface $Fe^{(II)}$ can neither be corroborated nor be excluded but it has been suggested that $Se^{(IV)}$ reduction to $Se^{(0)}$ is due to the oxidation of four $Fe^{(II)}$ surface groups, accompanied by a proton consumption (Scheinost and Charlet, 2008). This mechanism may only be marginal in the present study because it is not consistent with the observed formation of pyrite. Based on reported spectroscopic characterization of oxidized mackinawite (Bourdoiseau et al., 2008), it may also be possible that electrons needed to reduce $Se^{(IV)}$ were provided by $Fe^{(II)}$ from tetrahedral sites connected to surface sulfide groups.

Overall, surface sulfide groups contributed to the reductive immobilization $Se^{(IV)}_{aq}$, as indicated by the detection of FeS_2 . Even though the Se content was below the monolayer surface coverage, $Se^{(0)}$ was detected and indicates the formation of nanoparticulate elemental Se. It is very likely that such nanoparticles can be seen as "coating" and were only few angstroms in size (thickness) at maximum because S atoms were detected at 3.87(4) Å. The participation of $Fe^{(II)}$ in this retention may be likely, but no experimental evidence supports this hypothesis. Analysis of the sample by a surface sensitive technique such as X ray photoelectron spectroscopy was not attempted because of multiple overlaps of the binding energies (e.g., S 2s and Se 3s, S 2p and Se 2p, Fe 3p and Se 3d). The formation of solid solution like structure upon $Se^{(IV)}$ interaction with FeS can be discarded because only elemental selenium was detected and no Fe was detected in the Se first coordination sphere.

The data show that $Se^{(IV)}$ is reductively immobilized as nanoparticulate $Se^{(0)}$ at the surface of mackinawite upon oxidation of surface groups. Because this phase can potentially be present in the surrounding of HLW disposal sites, it may contribute to preventing Se migrating out of the repository. The data show that this may lead to the formation of pyrite, which is the most stable $Fe^{(II)}$ sulfide phase.

4. Conclusion

In this study selenite interacted with either $Fe^{(II)}_{aq}$ or $S^{(-II)}_{aq}$ in solution. In both experiments, $Se^{(0)}$ formed and the reaction mechanism could be identified. Results were also consistent with thermodynamic data. Selenite was also reduced to $Se^{(0)}$ upon interaction with FeS in suspension, and this solid contains $Fe^{(II)}$ and $S^{(-II)}$ sites that can reduce $Se^{(IV)}$. However, compared to reaction mechanisms determined for systems where $Se^{(IV)}$ interacted with either ferrous iron or sulfide, the data indicated that selenite was reduced by mackinawite at surface sulfide sites, which is also consistent with XRD data. All reduced species used in this study are expected to be present or to form in a HLW disposal site, and

thus it is very likely that Se^(IV) released from the waste matrix will be reductively immobilized in such facilities, thereby delaying the migration to the far field.

We could also show that investigations of systems involving only one oxidized and one reduced species can be used to identify reaction mechanisms for systems involving more than one reduced species responsible for reductive immobilization of redox sensitive pollutant. Depending on the reducing agent, it can be anticipated that the reaction may be kinetically slower because of the number of involved species. However, the presence of a mineral surface mediating the reaction can improve the rate of reaction e.g., by first retaining the reacting species at the surface before reducing the pollutant.

Acknowledgments

We thank E. Soballa (KIT INE) for SEM analyses. ANKA is acknowledged for provision of synchrotron radiation beam time. We thank an anonymous reviewer for comments which helped to improve the manuscript.

References

- Ankudinov, A.L., Ravel, B., et al., 1998. Real-space multiple-scattering calculation and interpretation of X-ray-absorption near-edge structure. *Phys. Rev. B* 58 (12), 7565–7576.
- Bourdoiseau, J.A., Jeannin, M., et al., 2008. Characterisation of mackinawite by Raman spectroscopy: effects of crystallisation, drying and oxidation. *Corros. Sci.* 50 (11), 3247–3255.
- Bouroushian, M., 2010. Electrochemistry of the Chalcogens. *Electrochemistry of Metal Chalcogenides*. Springer-Verlag, Berlin Heidelberg, pp. 57–75.
- Brostigen, G., Kjekshus, A., 1969. Redetermined crystal structure of FeS₂ (pyrite). *Acta Chem. Scand.* 23 (6) (2186-8).
- Charlet, L., Scheinost, A.C., et al., 2007. Electron transfer at the mineral/water interface: selenium reduction by ferrous iron sorbed on clay. *Geochim. Cosmochim. Acta* 71 (23), 5731–5749.
- Chen, Y.-W., Truong, H.-Y.T., et al., 2009. Abiotic formation of elemental selenium and role of iron oxide surfaces. *Chemosphere* 74 (8), 1079–1084.
- Cherin, P., Unger, P., 1967. The crystal structure of trigonal selenium. *Inorg. Chem.* 6 (8), 1589–1591.
- Cornell, R.M., Schwertmann, U., 1996. *The Iron Oxides: Structure, Properties, Reactions, Occurrences and Uses*. Springer, Weinheim.
- Dardenne, K., González-Robles, E., et al., 2015. XAS and XRF investigation of an actual HAWC glass fragment obtained from the Karlsruhe vitrification plant (VEK). *J. Nucl. Mater.* 460 (0), 209–215.
- Fernández-Martínez, A., Charlet, L., 2009. Selenium environmental cycling and bioavailability: a structural chemist point of view. *Rev. Environ. Sci. Biotechnol.* 8 (1), 81–110.
- Finck, N., Dardenne, K., et al., 2012. Selenium retention by mackinawite. *Environ. Sci. Technol.* 46 (18), 10004–10011.
- Finck, N., Dardenne, K., et al., 2015. Am(III) coprecipitation with and adsorption on the smectite hectorite. *Chem. Geol.* 409 (0), 12–19.
- Gaucher, É.C., Blanc, P., et al., 2006. Modelling the porewater chemistry of the Callovian–Oxfordian formation at a regional scale. *Compt. Rendus Geosci.* 338 (12–13), 917–930.
- Geoffroy, N., Demopoulos, G.P., 2011. The elimination of selenium(IV) from aqueous solution by precipitation with sodium sulfide. *J. Hazard. Mater.* 185 (1), 148–154.
- Giester, G., 1993. The crystal structure of Fe₂(SeO₃)₃·H₂O. *J. Solid State Chem.* 103 (2), 451–457.
- Hatten Howard III, J., 1977. Geochemistry of selenium: formation of ferroselite and selenium behavior in the vicinity of oxidizing sulfide and uranium deposits. *Geochim. Cosmochim. Acta* 41 (11), 1665–1678.
- Jörg, G., Bühnmann, R., et al., 2010. Preparation of radiochemically pure ⁷⁹Se and highly precise determination of its half-life. *Appl. Radiat. Isot.* 68 (12), 2339–2351.
- Kirsch, R., Fellhauer, D., et al., 2011. Oxidation state and local structure of plutonium reacted with magnetite, mackinawite, and chukanovite. *Environ. Sci. Technol.* 45 (17), 7267–7274.
- Lennie, A.R., Redfern, S.A.T., et al., 1995. Synthesis and Rietveld crystal structure refinement of mackinawite, tetragonal FeS. *Mineral. Mag.* 59 (397), 677–683.
- Libert, M., Bildstein, O., et al., 2011. Molecular hydrogen: an abundant energy source for bacterial activity in nuclear waste repositories. *Phys. Chem. Earth A/B/C* 36 (17–18), 1616–1623.
- Libert, M., Schütz, M.K., et al., 2014. Impact of microbial activity on the radioactive waste disposal: long term prediction of biocorrosion processes. *Bioelectrochemistry* 97, 162–168.
- Masscheleyn, P.H., Delaune, R.D., et al., 1990. Transformations of selenium as affected by sediment oxidation–reduction potential and pH. *Environ. Sci. Technol.* 24 (1), 91–96.
- Moyes, L.N., Jones, M.J., et al., 2002. An X-ray absorption spectroscopy study of neptunium(V) reactions with mackinawite (FeS). *Environ. Sci. Technol.* 36 (2), 179–183.
- Olin, A., Nolang, B., et al., 2005. *Chemical Thermodynamics of Selenium*. Elsevier Science, Amsterdam.
- Pettine, M., Gennari, F., et al., 2012. The reduction of selenium(IV) by hydrogen sulfide in aqueous solutions. *Geochim. Cosmochim. Acta* 83 (0), 37–47.
- Pickering, I.J., Brown, G.E., et al., 1995. Quantitative speciation of selenium in soils using X-ray absorption spectroscopy. *Environ. Sci. Technol.* 29 (9), 2456–2459.
- Ravel, B., Newville, M., 2005. ATHENA, ARTEMIS, HEPHAESTUS: data analysis for X-ray absorption spectroscopy using IFEFFIT. *J. Synchrotron Radiat.* 12, 537–541.
- Rickard, D., Griffith, A., et al., 2006. The composition of nanoparticulate mackinawite, tetragonal iron(II) monosulfide. *Chem. Geol.* 235 (3–4), 286–298.
- Rothe, J., Butorin, S., et al., 2012. The INE-beamline for actinide science at ANKA. *Rev. Sci. Instrum.* 83 (4).
- Scheinost, A.C., Charlet, L., 2008. Selenite reduction by mackinawite, magnetite and siderite: XAS characterization of nanosized redox products. *Environ. Sci. Technol.* 42 (6), 1984–1989.
- Scheinost, A.C., Kirsch, R., et al., 2008. X-ray absorption and photoelectron spectroscopy investigation of selenite reduction by FeII-bearing minerals. *J. Contam. Hydrol.* 102 (3–4), 228–245.
- Schlegel, M.L., Bataillon, C., et al., 2014. Corrosion of metal iron in contact with anoxic clay at 90 °C: characterization of the corrosion products after two years of interaction. *Appl. Geochem.* 51, 1–14.
- Schwertmann, U. and R. M. Cornell (1991). *Iron oxides in the laboratory preparation and characterization*, VCH Verlagsgesellschaft mbH: Weinheim, Germany; VCH Publishers, Inc.: New York, New York, USA.
- Weiss, J., 1977. Mitteilung über Interchalcogenverbindungen. IV. Röntgenographische Untersuchungen an Mischkristallen der Zusammensetzung SenS₈-n. *Z. Anorg. Allg. Chem.* 435 (1), 113–118.
- Wolthers, M., Van der Gaast, S.J., et al., 2003. The structure of disordered mackinawite. *Am. Mineral.* 88 (11–12), 2007–2015.
- Wolthers, M., Charlet, L., et al., 2005. Surface chemistry of disordered mackinawite (FeS). *Geochim. Cosmochim. Acta* 69 (14), 3469–3481.
- Zingaro, R.A., Carl Dufner, D., et al., 1997. Reduction of oxoselenium anions by iron(II) hydroxide. *Environ. Int.* 23 (3), 299–304.

Repository KITopen

Dies ist ein Postprint/begutachtetes Manuskript.

Empfohlene Zitierung:

Finck, N.; Dardenne, K.

[Interaction of selenite with reduced Fe and/or S species: An XRD and XAS study](#)

2016. Journal of Contaminant Hydrology, 188

[doi: 10.554/IR/1000055346](#)

Zitierung der Originalveröffentlichung:

Finck, N.; Dardenne, K.

[Interaction of selenite with reduced Fe and/or S species: An XRD and XAS study](#)

2016. Journal of Contaminant Hydrology, 188, 44–51.

[doi:10.1016/j.jconhyd.2016.03.001](#)